

Application of inverse SEA models to obtain the Coupling Loss Factor in structural junctions from numerical simulations

Poblet-Puig, Jordi¹

**Laboratori de Càlcul Numèric, Universitat Politècnica de Catalunya
E.T.S. d'Enginyers de Camins, Canals i Ports de Barcelona, Campus Nord B1,
Jordi Girona 1, E-08034 Barcelona**

Rodríguez-Ferran, Antonio²

**Laboratori de Càlcul Numèric, Universitat Politècnica de Catalunya
E.T.S. d'Enginyers de Camins, Canals i Ports de Barcelona, Campus Nord C2,
Jordi Girona 1, E-08034 Barcelona**

ABSTRACT

An inverse SEA procedure that mimics the Experimental SEA (ESEA) is used in order to obtain the Coupling Loss Factor (CLF) of structural junctions. The main differences with respect to ESEA are that: 1) the subsystem energies and input powers are obtained by means of numerical simulations; and 2) the internal damping is imposed and must not be determined a posteriori (which allows reorganisation of the equations). The numerical model is based on the Spectral Finite Element Method (SFEM). This helps in order to cover a large frequency range without increasing the number of elements and to efficiently perform a large number of simulations with different load configurations (both aspects are required by the inverse SEA procedure). The contribution analyses several aspects such as: various options to obtain the input power from the numerical model; possible modifications in the background SEA model in order to avoid negative CLF values; assessment of the validity of the SEA hypotheses; possible shortcuts in order to avoid matrix singularities or to deal with abundant data. Finally, it is shown how the CLF values obtained for simple configurations can be used to model the response of more complex structures.

Keywords: SEA, non-negative, vibration

I-INCE Classification of Subject Number: 76 (Modeling, prediction and simulation)
(see <http://i-ince.org/files/data/classification.pdf>)

¹jordi.poblet@upc.edu

²antonio.rodriguez-ferran@upc.edu

1. INTRODUCTION

Statistical Energy Analysis (SEA, [1]) is the most widely used modelling technique for vibroacoustic problems at high frequencies. It has been applied to building acoustics [2], train designs [3] or ships. The reliability of the simulation results depends on many different aspects. First of all, the SEA hypotheses must be satisfied [4]. Afterwards, the vibroacoustic system must be properly characterised. This implies performing an adequate definition of the subsystems (see for example [5]) and precisely characterising the input power, the internal losses and the energy transfers between them. The internal losses of a subsystem are characterised by the internal loss factor (ILF). It can be obtained from tables of material data and experiments. The energy transfers are characterised by the coupling loss factors (CLF). This is probably the key parameter in order to obtain a good SEA model of a vibroacoustic system. And it is not an easy task. Some expressions are available in the literature for the simplest connections. But there are no expressions for more complex situations. In those cases the use of numerical simulations ([6]) or experimental measurements is required.

The SEA parameters (ILF and CLF) can be determined by means of Experimental SEA (ESEA, see [7]). It mainly consists on the computation of SEA parameters from a set of experiments performed in the same SEA system. The energy of each subsystem and the input powers are measured. Afterwards the SEA parameters are obtained in an inverse way. It is inverse in the sense that the SEA parameters are usually known and used to predict the energies in each subsystem due to a given excitation (input power). And in ESEA the energies are the data and the ILF and CLF the outputs.

The main ESEA method is the power injection method. It requires to know the injected power in each subsystem. However some variations exist. For example [8] proposed a version of ESEA based on transfer matrices that does not require the knowledge or measurement of the input power.

ESEA procedures have been applied to multiple fields: building acoustics [9,10], noise produced by engines [11], application to a metallic box [12]. In fact, the idea behind ESEA methods can be considered also when the energies and the input powers are not obtained from experiments but from numerical simulations. We will refer here to Inverse SEA (ISEA) to talk in general about the idea of obtaining the ILF and CLF by means of an inverse algorithm whatever the origin of the energies is. A good example can be found in [13] where an ISEA procedure is used in order to obtain the CLF of two-dimensional junctions. The energies are obtained by means of the Spectral Finite Element Method (SFEM).

The advantages of ESEA are clear. It sometimes becomes the only way to estimate the CLF. This is more relevant in very complex systems and connections where semi-analytical models are not available and numerical models are difficult to develop (and the reliability of the results very limited by the drawbacks of standard numerical methods at high frequencies). However it has also important drawbacks. Some of them are related with the intrinsic difficulty of performing vibroacoustic experiments or the lack of repeatability of high-frequency measurements. But some others are directly related with the mathematical structure of the inversion algorithms. On the one hand, the matrices can often be very ill-conditioned. This depends on a poor definition of subsystems or the load configurations considered in order to perform the measurements. On the other hand, the error propagation can be very important leading to meaningless results. It was shown to be relevant even for very simple SEA problems composed by few subsystems [6].

The goals of the research are as follows:

1. Analysis of the ESEA methods, or inverse SEA (ISEA) methods in general.
2. Determine under which conditions can be ensured that the solution obtained with ISEA leads to positive CLF values. Relate existing linear algebra theorems with physical conditions on the vibroacoustic system and the SEA hypotheses.
3. Verify numerically the theoretical results
4. Apply the ISEA model to estimate the vibration transmission in an L-shaped junction.

2. METHODS

2.2.1. General SEA framework and notation

A brief review of the SEA equations is done here. More details can be found in [1, 14–16]. For a SEA system with N subsystems, the equilibrium of energy in every subsystem leads to

$$\omega \begin{bmatrix} \sum_{j=1}^N \eta_{1j} & -\eta_{21} & -\eta_{31} & \dots & -\eta_{N1} \\ -\eta_{12} & \sum_{j=1}^N \eta_{2j} & -\eta_{32} & \dots & -\eta_{N2} \\ \vdots & & \ddots & & \vdots \\ \vdots & & & \ddots & \vdots \\ -\eta_{1N} & -\eta_{2N} & -\eta_{3N} & \dots & \sum_{j=1}^N \eta_{Nj} \end{bmatrix} \begin{bmatrix} E_1 \\ E_2 \\ \vdots \\ \vdots \\ E_N \end{bmatrix} = \begin{bmatrix} \Pi_{in,1} \\ \Pi_{in,2} \\ \vdots \\ \vdots \\ \Pi_{in,N} \end{bmatrix} \quad (1)$$

where $\Pi_{in,i}$ is the power injected to the subsystem i , $\omega = 2\pi f$ is the pulsation of the problem, η_{ii} is the internal loss factor of the subsystem i , η_{ij} is the coupling loss factor between subsystems i and j , and E_i is the energy of the subsystem i .

The net power flow between subsystems i and j can be expressed as

$$\Pi_{ij}^{net} = \omega (\eta_{ij} E_i - \eta_{ji} E_j) \quad (2)$$

and the consistency relationship

$$\eta_{ij} n_i = \eta_{ji} n_j \quad (3)$$

must hold, where n_i is the modal density of the subsystem i .

2.2.2. Lalor formulation for ESEA [17]

The goal of ESEA is to determine the coefficients (ILF and CLF) of the matrix in the linear system of Equation 1. If the modal densities of the subsystems are unknown, there are N^2 coefficients (supposing that all subsystems are connected and modal densities unknown). In ESEA, the known information are the energies of the subsystems and the input powers (in the power injection version of the method). They are measured from an experiment (ESEA) or obtained from a numerical simulation (ISEA). At least N different experiments or load cases are required in order to be able to compute all the ILF and CLF. The N experiments must be done in order to obtain at least N^2 equations. They must be

as linearly independent as possible, and can be expressed in compact form as

$$\begin{bmatrix} \sum_{j=1}^N \eta_{1j} & -\eta_{21} & -\eta_{31} & \dots & -\eta_{N1} \\ -\eta_{12} & \sum_{j=1}^N \eta_{2j} & -\eta_{32} & \dots & -\eta_{N2} \\ \vdots & & \ddots & & \vdots \\ \vdots & & & \ddots & \vdots \\ -\eta_{1N} & -\eta_{2N} & -\eta_{3N} & \dots & \sum_{j=1}^N \eta_{Nj} \end{bmatrix} = \frac{1}{\omega} \begin{bmatrix} \Pi_{in,1}^1 & \dots & \Pi_{in,1}^N \\ \Pi_{in,2}^1 & \dots & \Pi_{in,2}^N \\ \vdots & & \vdots \\ \vdots & & \vdots \\ \Pi_{in,N}^1 & \dots & \Pi_{in,N}^N \end{bmatrix} \begin{bmatrix} E_1^1 & \dots & E_1^N \\ E_2^1 & \dots & \vdots \\ \vdots & & \vdots \\ \vdots & & \vdots \\ E_N^1 & \dots & E_N^N \end{bmatrix}^{-1} \quad (4)$$

where E_s^p is the energy in the subsystem s due to the load configuration p and $\Pi_{in,s}^p$ is the injected power in the subsystem s due to the load configuration p .

The inversion of the energies matrix shown in Equation 4 is not the most optimal way to perform the computation of η_{ij} . This can be a time consuming operation but also, and most relevant, a cause of error propagation. The error propagation is important here because the data obtained from experiments can have some inherent error (noise). A first strategy to overcome this difficulty is to choose the load configurations in such a way that the input power is

$$\Pi_{in,s}^p = \delta_{s,p} \Pi_{in} \quad (5)$$

with $\delta_{s,p}$ the Dirac-delta. This implies that only one subsystem is excited at each load configuration with the hope that

$$E_s^s \gg E_k^s \quad \text{for } \forall k \neq s \quad (6)$$

If this condition is satisfied, the spectral radius of the energies matrix should be smaller and the error propagation due to the inversion of the matrix less important.

Another option is to reorganise Equation 4 in such a way that a linear system of equations where the unknowns are the energies can be written. The explicit computation of an inverse matrix is no longer required (only the solution of a linear system). This option can be simplified if some CLF η_{ij} are null due to the definition of the SEA model. An example of this technique is shown in [10] for some SEA models of junctions. The limitation of this strategy is the possibility of rewriting the equations when a large number N of subsystems are involved.

Finally, the reorganisation of the equations proposed by Lalor in [17] is considered here. It splits the problem in $N - 1$ linear systems of $N - 1$ equations. They are expected to be better conditioned than the full energies matrix in Equation 4. The CLF are obtained first. Afterwards the ILF are computed as a post-process.

In the derivation of Lalor form of ESEA, the energy balance in the subsystem s due to the load configuration p must be considered:

$$\eta_s + \sum_{k=1, k \neq s}^N \left(\eta_{sk} - \frac{E_k^p}{E_s^p} \eta_{ks} \right) = \frac{\Pi_{in,s}^p}{\omega E_s^p} \quad (7)$$

A system of $(N - 1)$ equations can be obtained for every subsystem i in order to determine the coupling loss factors η_{ki} for $k = 1, 2, \dots, N$ and $k \neq i$. Each equation m is obtained by considering in the subsystem $s \equiv i$ the energy balance for the load case $p \equiv i$ minus the energy balance for the load case $p \equiv m$. Thus the generic equation is written as

$$\sum_{k=1, k \neq i}^N \left(\frac{E_k^m}{E_i^m} - \frac{E_k^i}{E_i^i} \right) \eta_{ki} = \frac{\Pi_{in,i}^m}{\omega E_i^m} \quad \text{for } m = 1, 2, \dots, N \text{ and } m \neq i \quad (8)$$

2.2.3. Analysis of positiveness of the CLF

It is a necessary condition (but not sufficient) that all the coupling loss factors $\eta_{ki} > 0$. This has the physical meaning that the power flows from the subsystem with more energy to the subsystem with less energy.

Thus the purpose of this section is to study under what conditions the non-negativity of all the CLF is satisfied by the $N - 1$ linear systems of equations 8. The problem has been analysed from an algebraic point of view in [18] where the following theorem is proven:

Theorem 1 Consider a linear system of M equations

$$\sum_{j=1}^M a_{ij}x_j = b_i \quad \text{for } i = 1, 2, \dots, M \quad (9)$$

with the following properties

$$a_{ii} > 0 \quad \text{for } i = 1, 2, \dots, M \quad (10)$$

$$a_{ij} \geq 0 \quad \text{for } i, j = 1, 2, \dots, M \quad \text{and } j \neq i \quad (11)$$

$$b_j \gg 0 \quad \text{for } j = 1, 2, \dots, M \quad (12)$$

If for all $i = 1, 2, \dots, M$, it is satisfied that

$$b_i > \sum_{j=1, j \neq i}^M a_{ij}b_j/a_{jj} \quad (13)$$

the linear system has a unique solution with all the coefficients larger than zero ($x_i > 0$ for $i = 1, 2, \dots, M$).

The previous theorem can be applied to the system in Equation 8. First of all, we need to study under which conditions the ESEA system 8 satisfy the requirements of the Theorem in Equations 10, 11 and 12.

The energy is a positive value. It is in general true that the excited subsystem has a much larger level of energy than the other subsystems. All together means that

$$\frac{E_m^m}{E_i^m} \gg 1 \quad (14)$$

which allows to ensure that the diagonal term ($k = m$ in Equation 8) of the matrix for the i^{th} group of CLF is largely positive

$$a_{mm} = \left(\underbrace{\frac{E_m^m}{E_i^m}}_{\gg 1} - \underbrace{\frac{E_m^i}{E_i^i}}_{\ll 1} \right) \gg 1 \quad \text{for } m, i = 1, 2, \dots, N \text{ and } m \neq i \quad (15)$$

this shows that the system in Equation 8 satisfies the condition 10.

If the difference in the energy level between the excited subsystem and any of the other subsystems is much larger than the energy difference between any pair of non-excited subsystems, for the out-of-diagonal terms we have

$$a_{mk} = \left(\frac{E_k^m}{E_i^m} - \frac{E_k^i}{E_i^i} \right) \gg 0 \quad \text{for } m, k, i = 1, 2, \dots, N \text{ and } m \neq i \text{ and } m \neq k \quad (16)$$

which satisfies condition 11. This is not true if a load configuration m causes null energy in subsystem k

$$E_k^m \equiv 0 \quad (17)$$

while a load configuration i causes non-null energy in subsystem k ($E_k^i > 0$, even if it is small). This situation will be commented later in the numerical examples.

Finally, the condition 12 is partially satisfied in the sense that

$$b_m = \frac{\prod_{in,i}^i}{\omega E_i^i} > 0 \text{ for } m = 1, 2, \dots, N \text{ and } m \neq i \quad (18)$$

but it is not clear to ensure that $b_m \gg 0$. In the limit for an isolated system i , b_m would be equal to the loss factor η_i which is a lower bound. But in general, the subsystem i has always other power flows which makes $b_m \gg \eta_i$.

A nice aspect is that b_m has the same values for all m and this allows a simplification of Equation 13

$$1 > \sum_{k=1, k \neq m}^M \frac{a_{mk}}{a_{kk}} \quad (19)$$

By excluding the cases when $E_k^m \equiv 0$, it can be assumed that

$$a_{mk} \approx \frac{E_k^m}{E_i^m} \quad \text{and} \quad a_{kk} \approx \frac{E_k^k}{E_i^k} \quad (20)$$

thus Equation 19 can be expressed as

$$1 > \sum_{k=1, k \neq m}^N \frac{E_k^m E_i^k}{E_k^k E_i^m} \quad \text{for } m, i = 1, 2, \dots, N \text{ and } m \neq i \quad (21)$$

As commented before, $\frac{E_k^m}{E_k^k}$ must be small ($\ll 1$) because the subsystem k will always have more energy when directly excited (in the load configuration k) than when another subsystem m is excited.

The term $\frac{E_i^k}{E_i^m}$ should be ≈ 1 if the subsystem i has similar levels of energy when any other subsystem is excited. This can be false when we have a very large problem with a lot of subsystems and most of the input power is lost in the path from k to i .

3. NUMERICAL EXPERIMENTS: STRUCTURAL JUNCTIONS

L-shaped and T-shaped junctions are considered in order to obtain the CLF with ISEA and illustrate some conclusion of the previous analysis. The numerical simulations are performed by means of the Finite Element Method (FEM) and the Spectral Finite Element Method (SFEM). Most of the details of this second numerical model can be found in [19].

In-plane and out-of-plane waves are modelled. The Uflyand-Mindlin theory ([20]) is considered to describe the bending behaviour.

The loss factor of the materials is assumed to be known. It is fixed as $\eta = 0.03$ here for the whole frequency range and all the wave types. This is mandatory in ISEA because the damping must be provided as data of the numerical model. And it simplifies quite a lot the ISEA analysis.

3.3.1. The SEA model of the L-junction

A general sketch of the SEA model for the L junction is shown in Fig. 1. Here, two different subsystem types are considered for every plate/shell. On the one hand the one which is representative of the out-of-plane displacements and the bending waves. For that case $E_i = M \langle |v_n|^2 \rangle / 2 = M \langle |v_{n,rms}|^2 \rangle$, where M is the total mass of the subsystem, v_n the phasor of normal velocity and the spatial average on the subsystem is considered.

On the other hand, the one which is representative of the in-plane displacements (grouped transverse and quasi longitudinal waves). In this case the energy is computed as $E_i = M \left(\langle |v_x|^2 \rangle + \langle |v_y|^2 \rangle \right) / 2$. Where v_x and v_y represent here the in-plane velocity phasors.

The couplings between subsystems are multiple (12). Essentially the following types are distinguished:

1. Between out-of-plane and in-plane subsystems in the same junction zone (pink)
2. Between out-of-plane and out-of-plane subsystems in different junction zones (green).
3. Between in-plane and in-plane subsystems in different junction zones (red).
4. Between out-of-plane and in-plane subsystems in different junction zones (blue).

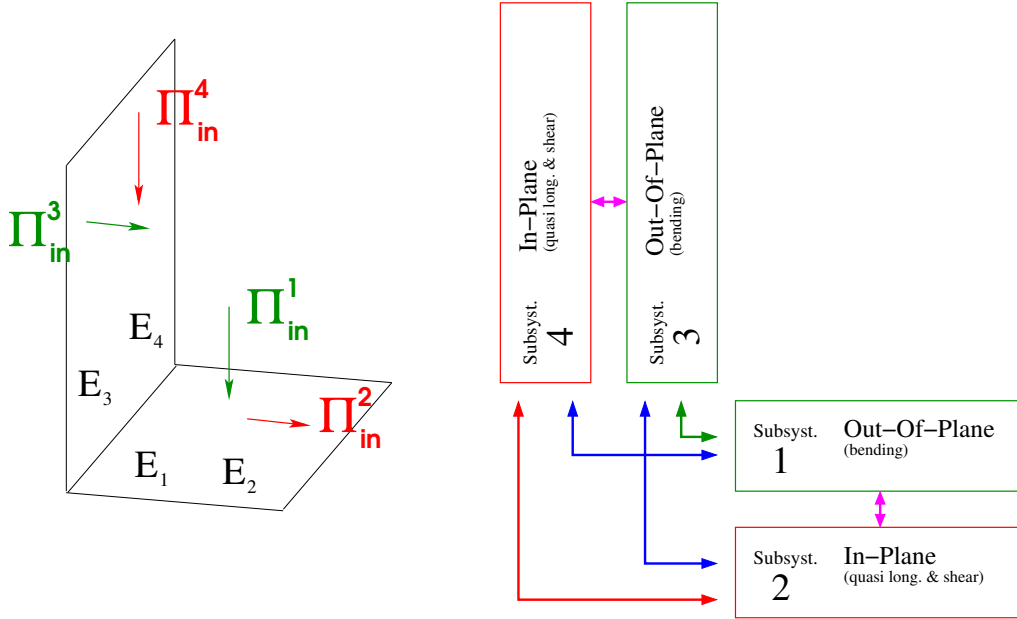


Figure 1: General SEA model for the L junction. It can consider four different subsystems: out-of-plane (subsystems 1 and 3) and in-plane (subsystems 2 and 4) for each region. All the possible connections between them are taken into account.

In order to perform the ISEA procedure, different load configurations need to be considered. For the L-junction, the four states of Fig. 1 are considered.

The power injected by a point force acting on a plate can be computed in two different ways. A first alternative is to use the definition of input power

$$\Pi_{in} = \frac{1}{2} \text{Re} \{ F v^* \} \quad (22)$$

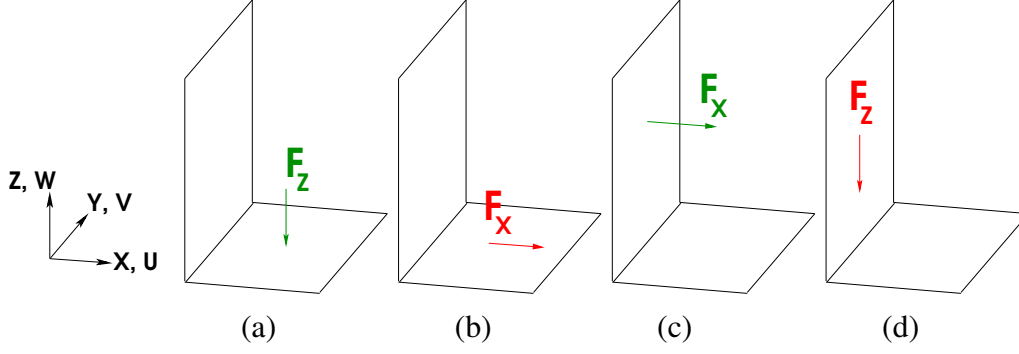


Figure 2: The four ESEA configurations for the L-junction model with four subsystems: (a) out-of-plane point force in the horizontal plate (floor position); (b) in-plane point force in the horizontal plate (floor position); (c) out-of-plane point force in the vertical plate (wall position); (d) in-plane point force in the vertical plate (wall position).

with F the phasor of the point force and v the phasor of the velocity at the application point, $*$ means complex conjugate. This formula is used for all type of point forces considered (out-of-plane and in-plane). The restriction is that v must be the velocity in the direction of the point force.

But since in the numerical simulations the loss factor is known (a big difference with the experiments), there is at least another way to estimate the input power

$$\Pi_{in} = \sum_i^N i\omega\eta_{ii}E_i \quad (23)$$

This is based on a global energy balance, assuming that the input power must be equal to the sum of the energy destroyed in all the subsystems. Note that this is possible because in the numerical simulations η_{ii} is known a priori.

3.3.2. Outputs for ISEA

In this section some examples of the outputs obtained with the numerical simulations are shown. They are the inputs of the ISEA process. The results are obtained with two different models: one based on FEM and the other on SFEM. Both simulations deal with the same junctions (L and T-shaped): dimensions, material properties, thicknesses of the plates, boundary conditions, zone of point force excitation. However, some differences inherent to each numerical technique exist. For example, the points used to make the spatial average of the vibration field in order to generate the output are not exactly the same. The point force that excites the structure is a nodal force in FEM while it must be represented as a narrow band (in space) force in SFEM (both forces with the same total magnitude). Also the interpolation field in the extrusion direction in SFEM is based on trigonometric functions, which is not the case in FEM. In spite of these small differences between the models, the results are very similar.

Fig. 3 shows a comparison between FEM and SFEM for a T-junction. In (a) we can see the spatially averaged in-plane velocity after a straight transmission between aligned elements when one of them is excited with an out-of-plane point force. In (b) we can see the spatially averaged out-of-plane velocity after a right-angle transmission between orthogonal elements when one of them is excited with an in-plane point force.

They are representative of all possible interactions between the SEA subsystems (load configuration versus subsystem energy).

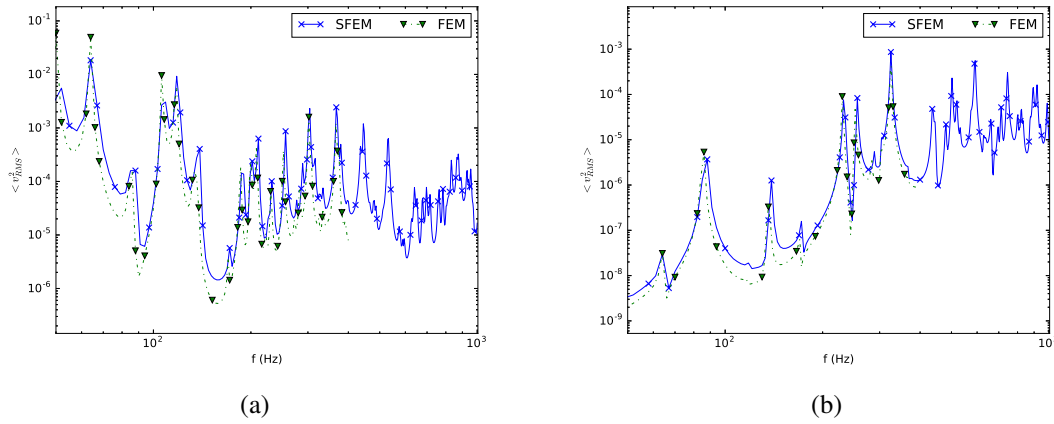


Figure 3: Vibration fields in a T-junction: (a) with point force orthogonal to the plate plane (it mainly generates bending), in-plane averaged velocity due to the straight transmission (to the front plate); (b) with point force in the plane of the plate (it generates mainly in-plane vibration), out-of-plane averaged velocity in the zone forming a right angle with the excited zone.

With the results in Fig. 3, the energies E_s^p can be computed. The other important aspect for the most popular versions of ESEA / ISEA is to determine the power injected to the subsystems. Fig. 4 shows how the injected power is obtained from the numerical model. Two possibilities are considered: using Equation 22 that considers the definition of injected power or using Equation 23 that considers a global balance of injected power and destroyed energies. From the numerical point of view, the first option requires an additional post-process of the results. But it reproduces better the experimental procedure. It is sensitive to the precision of the numerical model because the point where the force is applied tend to be in the zone of concentration of larger numerical errors. The second option, global balance of energies, is only valid if the SEA hypotheses are satisfied (because it is based on a SEA energy balance and not on the definition of input power). Consequently, the convergence of both methodologies to a single value of input power is an indirect indicator on the compliance of SEA hypotheses.

A first aspect to be noted is the similitude between the FEM and SFEM results. Fig. 3(a) shows the input power when the excitation is an out-of-plane point force. In that case the curves corresponding to the both procedures to measure the input power are similar even at low frequencies. It probably means that SEA hypotheses (concerning the input power) are early satisfied even at mid-low frequencies for this case. The density of bending modes is large. Fig. 3(b) shows the input power when the excitation is an in-plane point force. In this case the curves corresponding to the both procedures to measure the input power are only similar for frequencies higher that 300 Hz. It probably means that SEA hypotheses for subsystems modelling the in-plane vibrations are only satisfied at higher frequencies. This is probably due to the smaller modal density of modes involving in-plane displacement. At low and mid frequencies, very few of them can be found if compared to the bending modes.

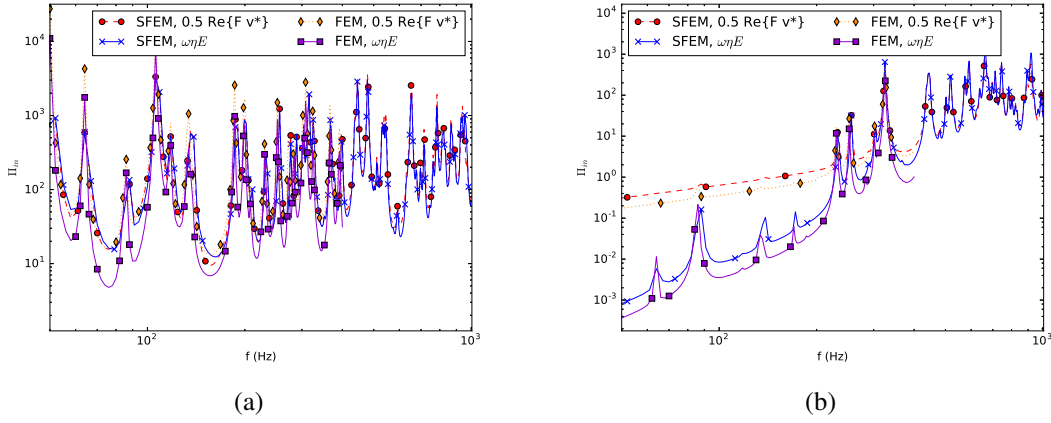


Figure 4: T-junction, simulation by means of FEM and SFEM. Input power due to the point force computed in different ways: (a) point force orthogonal to the plane of the left plate (it generates out-of-plane vibration); (b) point force in the plane of the plate (it generates mainly in-plane vibration).

3.3.3. Positiveness of the CLF

The ISEA analysis applied to the L-shaped junction illustrates the problem with negative values of the CLF. A large population of junctions have been considered, with variations on: the material properties, the thicknesses and the plate dimensions (specific data can be found in [21]). The result shown here are illustrative for most of the tested cases.

Fig. 5 contains the CLF obtained when all possible couplings between subsystems are allowed. It shows the CLF $\eta_{2,1}$, coupling between in-plane and out-of-plane subsystems in the first plate; and $\eta_{3,4}$ coupling between out-of-plane and in-plane subsystems in the second plate averaged in third-octave frequency bands. For many of the bands the symbol is not shown or there is a vertical line. This means that the CLF is negative. This also happens for $\eta_{1,2}$ and $\eta_{4,3}$. It is for all the CLF between out-of-plane and in-plane subsystems in the same plate. This is of course not desired. The cause is that the energies $E_1^2, E_2^1, E_3^4, E_4^3$ are null or almost null. When one of these subsystems is directly excited, almost no energy flows to the other. This is the ESEA drawback explained in Equation 17.

The linear systems to be solved can be almost singular or every ill conditioned. The CLF tend to zero (much smaller than the other CLF values) or oscillate between positive and negative values. This happens more often for low frequencies.

In order to overcome this drawback, a reformulation of the ESEA procedure for the L-junction is considered. It consists mainly in the determination a priori of the less important CLF and neglect them from the very beginning.

4. CONCLUSIONS AND FUTURE WORK

An analysis on the positiveness of the CLF values obtained as output of an ESEA process is done. Some tasks are pending on this research:

- Check the dependence of the CLF on the ILF. For the moment all the analysis has been done with $ILF = 0.03$.

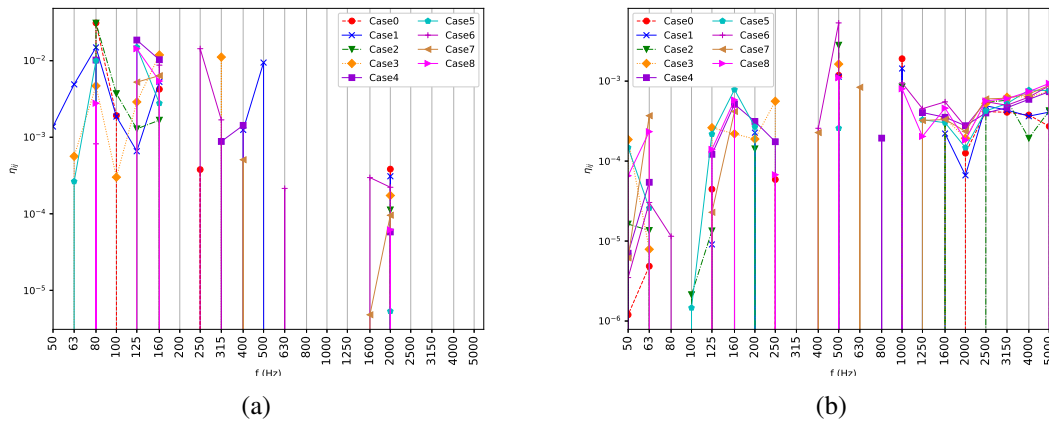


Figure 5: CLF obtained by means of the ISEA procedure applied to an L-junction: (a) $\eta_{2,1}$; (b) $\eta_{3,4}$. Each case correspond to different junction dimensions.

- Analysis of the performance of the ESEA / ISEA techniques in this context and if possible propagation of errors.
- Analyse the applicability of the obtained CLF to the simulation of a larger problem.
- Discussion on the different ways to compute the input power caused by a point force. Use it as a systematic verification of the SEA hypotheses.

5. ACKNOWLEDGEMENTS

LaCàN research group is grateful for the sponsorship/funding received from Generalitat de Catalunya (Grant number 2017-SGR-1278). The authors also appreciate the support of the project DPI2016-74929-R.

6. REFERENCES

- [1] R.H. Lyon and Richard G. DeJong. *Theory and application of statistical energy analysis*. Butterworth-Heinemann, 1995.
- [2] C. Hopkins. *Sound insulation*. Butterworth-Heinemann, 2012.
- [3] J. Forssén, S. Tober, A. C. Corakci, A. Frid, and W. Kropp. Modelling the interior sound field of a railway vehicle using statistical energy analysis. *Applied Acoustics*, 73(4):307–311, 2012.
- [4] T. Lafont, N. Totaro, and A. Le Bot. Review of statistical energy analysis hypotheses in vibroacoustics. *Proc. R. Soc. A*, 470(2162):20130515, 2014.
- [5] C. Díaz-Cereceda, J. Poblet-Puig, and A. Rodríguez-Ferran. Automatic subsystem identification in statistical energy analysis. *Mech. Syst. Signal Proc.*, 54-55:182–194, 2015.

- [6] C. Díaz-Cereceda, J. Poblet-Puig, and A. Rodríguez-Ferran. Numerical estimation of coupling loss factors in building acoustics. *J. Sound Vibr.*, 332(21):5433–5450, 2013.
- [7] B. Cimerman, T. Bharj, and G. Borello. Overview of the experimental approach to statistical energy analysis. SAE International, 1997.
- [8] O. Guasch. A direct transmissibility formulation for experimental statistical energy analysis with no input power measurements. *J. Sound Vibr.*, 330(25):6223–6236, 2011.
- [9] C. Hopkins. Statistical energy analysis of coupled plate systems with low modal density and low modal overlap. *J. Sound Vibr.*, 251(2):193–214, 2002.
- [10] C. Hopkins. Experimental statistical energy analysis of coupled plates with wave conversion at the junction. *J. Sound Vibr.*, 322(1-2):155–166, 2009.
- [11] L. Wu and A. Ågren. Applicability of the experimental statistical energy analysis to an engine structure. 1995.
- [12] J.C. Sun and E.J. Richards. Prediction of total loss factors of structures, I: Theory and experiments. *J. Sound Vibr.*, 103(1):109–117, 1985.
- [13] K.M. Ahmida and J.R.F. Arruda. Estimation of the SEA coupling loss factors by means of spectral element modeling. *Journal of the Brazilian Society of Mechanical Sciences and Engineering*, 25(3):259–263, 2003.
- [14] R.H. Lyon. *Statistical energy analysis of dynamical systems: theory and applications*. MIT press Cambridge, 1975.
- [15] M. P. Norton and D.G. Karczub. *Fundamentals of noise and vibration analysis for engineers*. Cambridge university press, 2003.
- [16] A. Le Bot. *Foundation of Statistical Energy Analysis in Vibroacoustics*. Oxford, 2015.
- [17] N. Lalor. The experimental determination of vibrational energy balance in complex structures. In *Stress and Vibration: Recent Developments in Industrial Measurement and Analysis*, volume 1084, pages 302–315. International Society for Optics and Photonics, 1989.
- [18] M. Kaykobad. Positive solutions of positive linear systems. *Linear algebra and its applications*, 64:133–140, 1985.
- [19] J. Poblet-Puig and C. Guigou-Carter. Using spectral finite elements for parametric analysis of the vibration reduction index of heavy junctions oriented to flanking transmissions and EN-12354 prediction method. *Appl. Acoust.*, 99:8–23, 2015.
- [20] I. Elishakoff, F. Hache, and N. Challamel. Vibrations of asymptotically and variationally based uflyand–mindlin plate models. *International Journal of Engineering Science*, 116:58–73, 2017.
- [21] C. Hopkins, C. Crispin, J. Poblet-Puig, and C. Guigou-Carter. Regression curves for vibration transmission across junctions of heavyweight walls and floors based on finite element methods and wave theory. *Appl. Acoust.*, 113:7–21, 2016.